

PAPER • OPEN ACCESS

## Steady state and a general scale law of deformation

To cite this article: Yan Huang 2017 *IOP Conf. Ser.: Mater. Sci. Eng.* **219** 012029

View the [article online](#) for updates and enhancements.

### Related content

- [Modeling the effect of deformation on strength of a Fe-23Mn-0.3C-1.5Al TWIP steel](#)  
P Kusakin, A Belyakov, R Kaibyshev et al.
- [Superstrength of nanostructured alloys produced by SPD processing](#)  
R Z Valiev, N A Enikeev and X Sauvage
- [High strength state of UFG steel produced by severe plastic deformation](#)  
N A Enikeev, X Sauvage, M M Abramova et al.

# Steady state and a general scale law of deformation

Yan Huang

BCAST, Brunel University London, Uxbridge, UB8 3PH UK

Email: [yan.huang@brunel.ac.uk](mailto:yan.huang@brunel.ac.uk), Tel: +44 1895 266976

**Abstract.** Steady state deformation has been characterized based on the experimental results for dilute single-phase aluminium alloys. It was found that although characteristic properties such as flow stress and grain size remained constant with time, a continuous loss of grain boundaries occurred as an essential feature at steady state. A physical model, which takes into account the activity of grain boundary dislocations, was developed to describe the kinetics of steady state deformation. According to this model, the steady state as a function of strain rate and temperature defines the limit of the conventional grain size and strength relationship, i.e., the Hall-Petch relation holds when the grain size is larger than that at the steady state, and an inverse Hall-Petch relation takes over if grain size is smaller than the steady state value. The transition between the two relationships relating grain size and strength is a phenomenon that depends on deformation conditions, rather than an intrinsic property as generally perceived. A general scale law of deformation is established accordingly.

## 1. Introduction

From early studies on face-centred cubic (fcc) crystalline metals and alloys it is known that stress-strain curves exhibit well-defined stages and microstructure dependencies [1-3]. Extensive investigations have been conducted since that time to verify, characterize and model the mechanical response and microstructural evolution in different stages of deformation. One of the widely addressed topics is work hardening behaviour, from the initial hardening stage (stage I) in association with easy glide by single slip and/or inhomogeneous slip due to Piobert-Lüders band propagation, to athermal linear hardening (stage II) and dynamic recovery related hardening (stage III and IV) [4-6]. Plasticity of crystalline materials is traditionally separated into two regimes, namely cold deformation at one end and hot deformation, including creep, at the other. Although the hardening in stage II does not usually take place at elevated temperatures, for both conditions the resistance to plastic deformation, i.e., flow stress ( $\sigma$ ) and strain rate ( $\dot{\epsilon}$ ) at a given temperature ( $T$ ), reaches a steady state. In some metals and alloys, such as copper, nickel, and austenitic steels, stress oscillation may occur in the early stages of deformation due to recrystallization, but a steady state eventually follows and prevails. Irrespective of whether dynamic recrystallization occurs, the strain rate and temperature dependence of the steady-state stress is often described by an empirical equation [7, 8]:

$$\dot{\epsilon} = A(\sinh \alpha \sigma)^n \exp\left(-\frac{Q}{RT}\right), \quad (1)$$

where  $A$ ,  $\alpha$  and  $n$  are temperature-independent constants, and  $Q$  is the activation energy. At low homologous  $T$  and high  $\sigma$ , equation (1) reduces to a power relation,



$$\dot{\epsilon} = A' \sigma^n \exp\left(-\frac{Q}{RT}\right) \quad (2)$$

Similarly at high stresses it equation (1) reduces to an exponential relation

$$\dot{\epsilon} = A'' \exp(\beta\sigma) \exp\left(-\frac{Q}{RT}\right) \quad (3)$$

The constants  $\alpha$  and  $n$  are related by  $\beta = \alpha n$ . The transition between the high and low  $T$  regimes is called power-law breakdown, which is generally explained by the transition in the governing kinetics of dislocation storage and annihilation from climb at high  $T$  to glide-controlled spontaneous behaviour at low  $T$ . It is worth noting that the steady state is usually difficult to achieve under conventional tensile testing conditions since sample typically fail by cracking or necking before reaching this stage, but it can generally be achieved under hot rolling or torsion conditions. Creep is a case where a steady state can be obtained, particularly at elevated temperatures. In the last two decades, the exploitation of severe plastic deformation technologies has made it clear that steady state deformation occurs exclusively even at the liquid nitrogen temperature [9, 10].

It is often observed that the average dislocation density and subgrain size are constant with straining at the steady state [11]. There have been a number of models describing the evolution of microstructures at the steady state. For instance, the model proposed by Mecking and Kocks [12] and the one developed by Gottstein and Argon [13] predict the average dislocation density and the flow stress at the steady state of both constant strain rate test and creep test. A three parameter approach proposed by Nes [5] and Marthinsen and Nes [14] describes the steady state in terms of the subgrain size, the dislocation density inside the subgrains, and the subgrain boundary dislocation density or the subgrain boundary misorientation. There are also models that take into account dynamic recrystallization in the deformation processes, which involve stress oscillation due dynamic recrystallization [15-17]. An essential assumption in all these approaches is that the dislocation density at steady state is constant.

Although the steady state microstructure only depends on the instantaneous values of strain rate and temperature, not on their history, the dynamic response of microstructure to strain on the pathway to the steady state is strongly dependent on the characteristic grain size of the material. For coarse-grained materials, the yield stress is inversely proportional to the square root of grain size as described by the famous Hall-Petch (H-P) relationship [18,19]. The relationship holds for a wide range of polycrystalline materials with grain sizes ranging from the millimetre scale down to the sub-micrometer scale, and also holds for the dependence of flow stress on the deformed grain/subgrain structure during deformation [20]. However, an inverse H-P relationship has also been reported for nano-grained materials [21, 22], where the strength of material is found to decrease with a decreasing grain size. Evidence for this switch from a normal H-P relationship to an inverse H-P relationship has been frequently observed in nanograined materials and it is widely accepted that the inverse H-P relationship is related to the intrinsic behaviour of crystalline materials as the grain size approaches a true nanoscale [23-26]. The explanation of the two regimes for the strength and grain size relationship has been mainly associated with the “high energy” character and high volume fraction of grain boundaries at nanoscale. The switchover from one regime to the other is often arbitrarily related to an absolute grain size rather than rationalized through mechanism analysis.

Steady state deformation presents a dynamic but definite correlation between flow stress and microstructure. This is probably the main reason for its attraction to materials scientists as it is amenable to detailed microstructural analysis and mathematical modelling. However, the nature for the establishment of a steady state is not properly understood, the characteristic microstructural features are not properly described and its fundamental importance is ignored. This paper aims to demonstrate that the essential and widely accepted assumption that the steady state is determined by a balance between dislocation accumulation due to work hardening and elimination due to dynamic recovery, based on which most analyses and modelling of steady state deformation are developed, is incorrect. A new model of steady state deformation will be put forward in consideration of the operation of grain boundary dislocations, which further leads to the establishment of a scale law of deformation.

## 2. Grain boundary loss at steady state

Steady state deformation occurs as a dynamical balance between the applied stress and microstructure is approached, where the microstructure is characterized by a constant grain/subgrain size and constant dislocation density. However, the total grain boundary area is not constant and, in fact, there is a constant loss of grain boundaries at steady state. This phenomenon has been long observed and recognized [27] but its paramount importance is overlooked and ignored in understanding the active deformation mechanisms. In plastic deformation, there is always a loss of dislocations from the interior to the surface, which makes the physical deformation possible. At steady state, the widely accepted concept that the generation of dislocation due to deformation is balanced by dynamic recovery leads to the miscalculation of a significant amount of dislocations. The amount of discrepancy is the total amount of dislocations moved out to the surface.

Geometrically, grains are required to change shape in proportion to the external shape change during plastic deformation. In the case of plane strain compression (PSC), for example, the geometrically required grain size in the compression direction ( $D_G$ ) can be related to its initial value of  $D_0$  and the accumulative true strain ( $\epsilon_t$ ) by [28]

$$D_G = D_0 \exp(-\epsilon_t) \quad (4)$$

The actual grain size tends to follow the above relation in the early stages of deformation, particularly at cryogenic temperatures, but rapidly deviates from it at high strains. Steady state deformation is an extreme condition where grain size remains constant and independent of strain. This means that there must be a loss of grain boundaries in order to compensate the grain size reduction due to geometrical compression described by Equation 4. The fraction of the lost HAB area ( $f_L$ ) relative to the initial grain boundary area is determined by the total strain ( $\epsilon_t$ ),

$$f_L = 1 - \left(\frac{D_0}{D}\right) \exp(-\epsilon_t), \quad (5)$$

where  $D$  is the instantaneous grain size. The grain boundary area loss at steady state is

$$f_L = 1 - \exp(-\epsilon_s) \quad (6)$$

where  $\epsilon_s$  is the accumulative strain at the steady state. It can be extrapolated from equation (6) that at very high strains,  $f_L$  is close to 1, i.e. most grain boundaries are eliminated from the material. This can be understood by envisaging a case where the workpiece thickness is equal to the grain size and there are no grain boundaries between the surfaces, except those aligned parallel to the compression direction.

The constant dislocation density assumption apparently can neither explain the constant grain structure nor the loss of grain boundaries. Thermally activated competitive coarsening between grains may do and needs to be examined. In order to remain at a constant grain size, grain boundaries must migrate during deformation at a rate equal to that of their compression,  $V_C$ , which can be related to strain rate,  $\dot{\epsilon}$ , by

$$V_C = dD/dt = D\dot{\epsilon} \quad (7)$$

The analysis of data obtained from an Al-0.1Mg alloy showed that the velocity was significantly too high to be explained by any possible mechanisms of grain boundary migration [29, 30]. In a previous study, an Al-0.1Mg alloy was firstly deformed to a true strain of 10 by equal channel angular extrusion at room temperature and then deformed by PSC to strains where a steady state was well established at temperatures from 77K to 473K and at a strain rate of  $10^{-2} \text{ s}^{-1}$ . The steady state grain size was measured by EBSD and the “boundary migration rate” was estimated according to equation (7), which is plotted against inverse temperature in figure 1. In the range of 77-273K, the apparent activation energy, determined from the slope of this plot, was as low as  $\sim 1 \text{ kJ mol}^{-1}$ . Above 373K the slope gives an activation energy of  $\sim 60 \text{ kJ mol}^{-1}$ . Velocities predicted by all possible boundary migration mechanisms, including curvature driven, stress and vacancy assisted migration and solute breakaway mechanism, are also plotted in the figure but none of these fit the measured values.

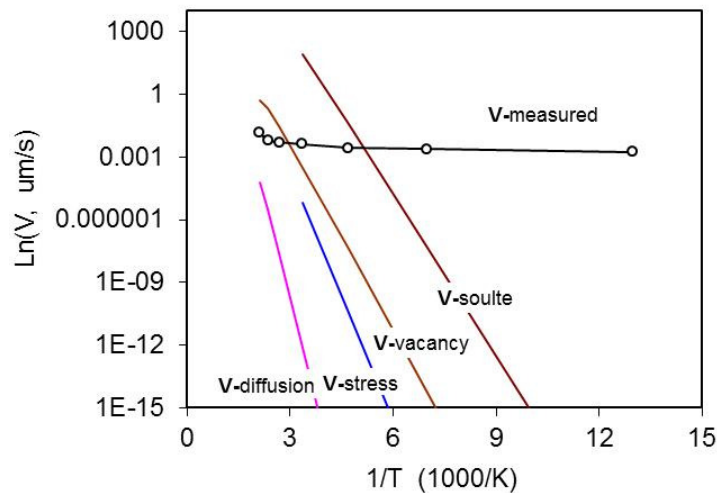


**Figure 1.** Estimated high angle boundary migration rate in the compression direction as a function of reciprocal temperature during PSC of an Al-0.1Mg alloy.

The boundary migration rate ( $V$ ) is usually assumed to be proportional to the driving pressure ( $P$ ), i.e.,  $V = MP$ , where  $M$  is the boundary mobility. For conventional diffusion controlled boundary migration driven by boundary curvature [11],

$$V = \frac{\gamma}{4r} M_0 \exp\left(-\frac{Q}{RT}\right), \quad (8)$$

where  $r$  is the radius of curvature,  $\gamma$  the boundary energy,  $M_0$  the mobility coefficient and  $Q$  the activation energy. Using parameters determined from static grain growth experiments at 423–773K for the same alloy ( $M_0 = 0.1 \text{ m}^4\text{J}^{-1}\text{s}^{-1}$ ,  $Q = 130 \text{ kJmol}^{-1}$ ) [31, 32], taking  $\gamma = 0.32 \text{ J/m}^2$  and  $r = D/2$ , velocities calculated from equation (8) are lower than the experimentally determined rates ( $V_C$ ) by a factor of  $10^{10}$  at 298K, and by progressively larger amounts at lower temperatures, being  $\sim 10^{74}$  times slower at 77K. The effect of elastic energy differences between neighbour grains has been discounted in the literature due to the low anisotropy of Al crystals. Estimates using variations in the Taylor factor result in a driving pressure 10-30 times below that due to boundary tension. Equally, dislocation density is low in ultra-fine grained materials and does not provide a significant additional pressure for boundary migration. In any event, no realistic increase in the average driving pressure can account for the many orders of magnitude difference in boundary migration rates between observations and predictions at low temperatures. It has been claimed that high transient vacancy concentrations can be generated during severe deformation [33, 34] and enhance boundary migration. However, an abundant flux of vacancies would only reduce the vacancy formation part of the activation energy [35] and cannot explain the behaviour below room temperature. An additional possibility is that highly disordered grain boundary structures under dynamic conditions could have increased boundary mobility [36]. However, much higher apparent activation energies should be observed if such effects took place substantially.

Overall, none of the above reviewed mechanisms can explain the measured dynamic recovery rate, particularly at low temperatures. The conventional thermally activated boundary migration model therefore seems inappropriate under these conditions.

### 3. Grain boundary dislocation in operation

The operation of grain boundary dislocations is considered to be a feasible mechanism that can explain both the deformation and microstructural evolution at steady state. Dislocation emission from GBs is a long recognized and an experimentally verified phenomenon [37-41]. GB dislocation emission can lead to the decrease in boundary misorientation and even the elimination of the boundary. The merging of two adjacent grains due to orientation convergence can be an example of this, which gives

rise to the development of textures, in addition to well addressed dislocation density dependency of the misorientation of low angle boundaries [11].

Figure 2 shows microstructural evolution during *in-situ* tensile deformation at 315°C and  $2.5 \times 10^{-4} \text{ s}^{-1}$  in an Al-0.05Si alloy that was previously deformed in compression in a channel die to a reduction of 70% at 300°C. The electron backscatter images in figure 2 were taken from the same area during deformation between strains of 0.24 to 0.28, where steady state deformation was established. In this small strain interval, grain coalescence and subdivision is observed together with other features such as grain rotation. It can be seen from the figure that grain boundaries A and B disappeared *in-situ* without the involvement of migration and grain C was subdivided into several grains. The two mechanisms operated simultaneously and the steady state was maintained. The range of boundary misorientation involved was not clear but the observation confirms that strain-induced misorientation reduction and boundary elimination does occur.

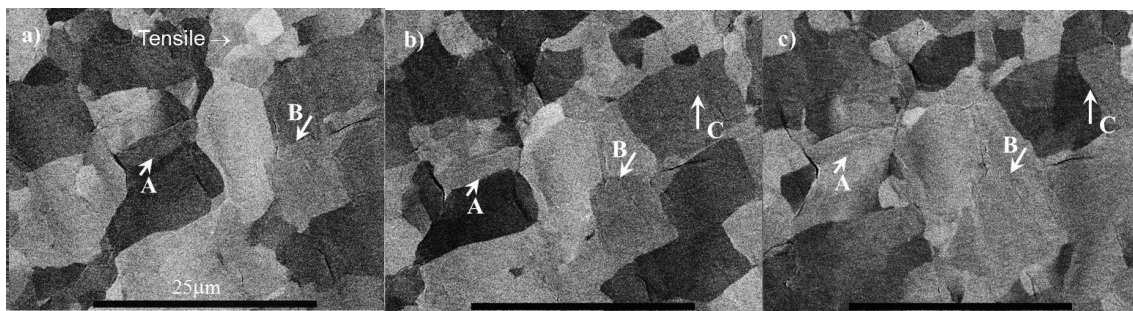


**Figure 2.** Electron backscattered images of grain structures taken from the same area during steady state deformation of an Al-0.05Si alloy at 315°C and  $2.5 \times 10^{-4} \text{ s}^{-1}$  to strains of: a) 0.24, b) 0.26 and c) 0.28.

#### 4. A new model of steady state deformation

It is the author's hypothesis that GB dislocation emission takes place at all stages of deformation including initial yielding. Before approaching steady state, dislocations emitted from grain boundary sources interact with dislocations inside grains and other obstacles. Their further glide and multiplication is controlled by the Frank-Read source mechanism [42]. The flow stress is primarily determined by the dislocation mean free path  $L$ , which is the distance travelled by a dislocation segment of a certain length before it is stored by interaction with the microstructure [43],

$$\tau = \tau_0 + \alpha Gb/L \quad (9)$$

where the constant  $\alpha = 1$  for edge dislocations and 0.5 for screw dislocations,  $G$  is the shear modulus and  $b$  the Burger's vector. The mean free path,  $L$ , is related to average dislocation density ( $\rho$ ) by  $\rho = L^{-2}$ . Apparently, if  $L$  and the square root grain size are linearly correlated, the observed H-P relationship can be explained more straightforwardly.

At the steady state, the dislocation mean free path and average grain size are convergent and the former reaches its minimum. For grains that are smaller than the average size, dislocation multiplication from a F-R source is not possible because the applied stress cannot overcome the tension of a dislocation segment that is smaller than the minimum dislocation mean free path. Dislocations emitted from grain boundary will be free to glide. The boundary dislocations are ultimately pushed into the surface of the material and consequently deformation takes place. As discussed above, a grain boundary reduces its misorientation and vanishes as a result of dislocation emission. The elimination of grain boundary due to dislocation emission will result in grain size increase, compensating the effect of external shape change. On the other hand, grains that are larger than the average steady state size can still accommodate F-R sources and deformation is dominated by dislocation glide and multiplication via the bowing out mechanism from the F-R sources. Their sizes decrease following equation (3) approximately if no new boundaries are generated within them. It is thus the balance between the operation of intragranular and GB dislocation sources that gives rise to a

constant grain structure at the steady state. A new model of steady state is therefore proposed with the features described below.

- The steady state is the ultimate destination of flow stress and microstructure.
- The average grain size at the steady state ( $D_s$ ) is determined by the minimum dislocation mean free path for given strain rate and temperature.
- There is always a distribution in grain size. For grains  $D > D_s$ , F-R sources operate while for grains  $D < D_s$ , GB dislocation sources dominate.
- The operation of F-R sources results in the decrease in grain size, while the operation of GB dislocations leads to the loss of GBs and an increase in grain size.
- F-R and GB sources are balanced, giving rise to a constant flow stress and grain size.

### 5. A new model of GB dislocation glide

It is proposed that a segment of dislocation emitted from grain boundary glides by the migration under the applied stress of its terminating points at the grain boundary or grain boundaries, from which it originates, i.e. its GB ends,. This is a new mechanism for dislocation movement, only suitable for GB dislocation sources as there is no involvement of dislocation multiplication in the process. Figure 3 shows the essential elements involved in this dislocation glide process, including a segment of dislocation line L ending at grain boundary points A and B, and intersecting with the grain boundary at an angle ( $\beta$ ), the half opening angle relative to the dislocation glide direction ( $\phi$ ), and the curvature

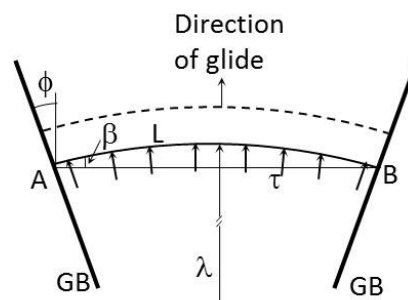


**Figure 3.** Geometrical model of dislocation glide by the migration of its GB ends.

of the dislocation line ( $\lambda$ ). The glide of a dislocation in the configuration depicted in figure 3 will result in the extension of the dislocation line. Since under a given applied stress the curvature of the dislocation line will remain constant, the extension of the dislocation will be realized only by transforming the GB dislocation into the grain. If the angle  $\phi$  is negative, alternatively, which is realistically possible, the dislocation line will retract as the dislocation sinks into grain boundary. . The dislocation, including its GB ends, should have the same Burgers vector with the same combination of edge and screw components along its line. With the help of the principle of virtual work, the stress required to operate the dislocation segment by the migration of its GB ends can be derived as a function of geometrical and material parameters and a simplified relation is given as

$$\tau = \tau_r + \frac{2w}{L} \tau_r^{gb} - \frac{\alpha G b}{\lambda} \frac{2c-L/\lambda}{L}, \quad (10)$$

where  $\tau_r$  is the stress required to overcome lattice, solute and other distribution resistances inside the grain,  $w$  is the width of grain boundary,  $\tau_r^{gb}$  is the stress required to overcome resistance from the GB ends of the dislocation, and  $c = 1 + \sin\beta - \phi$  is a geometrical factor. The length of dislocation segment  $L$  is of the same scale as the grain size and its curvature  $\lambda$  is always larger than the steady state grain size. If  $2c-L/\lambda$  is positive, which is safely met when  $\phi$  is less than 0.5, the third term on the right hand side of equation (10) will be positive itself and it increases with decreasing  $L$  or grain size. Thus equation (10) predicts a proportional relationship between flow stress and grain size, i.e. that the stress increases with increasing grain size.

The model presented here demonstrates the basic concept of GB dislocation operation as a key mechanism of deformation at steady state, or in the pathway to the steady state, when the grain size is smaller than the steady state size. There are, however, several fundamental issues yet to be addressed to complete the full picture of this process. These include the activation and initiation of GB dislocations, and the relationship between GB dislocation density and misorientation. The annihilation of GB dislocations must occur, but dislocation emission is considered to contribute to deformation. There is also an issue whether all GBs are consumable by dislocation emission/annihilation as not all of them are “dislocation boundaries”. Indeed, most GBs cannot be simply constructed by the configuration of dislocations as basic elements. However, the total loss of GB area in the Al-0.1Mg alloy deformed at room temperature by PSC to a true strain of 2.8, as part of the investigation on the same alloy as described above, was estimated by equation (5) to be about 90%. It is thus not unreasonable to assume that all GBs are consumable by dislocation operation.

### 6. A universal scale law of deformation

Equation (10) is considered to be a special form of an inverse Hall-Petch relationship, with respect to the dependence of material strength on grain size at its lower end. It has been widely claimed that an inverse H-P relationship only occurs when the grain size is refined to a real nanoscale, for example 10 nm. Logically, it is unconvincing to describe a behavioural change as a function of scale using the scale as a criterion. Actually, a strength-grain size dependence similar to the inverse H-P relation has been observed in creep and superplastic flow where the grain size covers a wide range of scales from nanometres to millimetres. Investigations on this topic have not yet produced convincing evidence to demonstrate substantial differences for the proportional strength and grain size relationships observed in monocrystalline materials and most other situations such as creep and superplastic deformation.

It is generally accepted and also the basis of the present discussion that dynamic responses of microstructure to plastic deformation are strongly dependent on grain size. Grain subdivision takes place during deformation of coarse grained materials, whereas equation (10) suggests that, starting from the other end with a grain structure smaller than that of the steady state, grain structure coarsening occurs during deformation. Equation (10) has a universal nature as it suggests that the switchover point, which is at the steady state, is determined by the deformation conditions, mainly strain rate and temperature but actual grain size, instead of concrete grain size. For a certain starting grain size, hardening occurs if the steady state size defined by the applied strain rate and temperature is smaller; otherwise, softening takes place.

### Summary

A novel description of steady state deformation is provided in light of grain boundary loss with the support of experimental evidence obtained from the severe plastic deformation of an Al-0.1Mg alloy and SEM in-situ straining of an Al-0.05Si alloy. An analytical model of novel dislocation glide mechanism via the migration of grain boundary ends is proposed, which leads to the establishment of a universal scale law of deformation.

### Acknowledgments

Financial support from EPSRC LiME Hub (UK) is gratefully acknowledged.

### References

- [1] Mitchell T E 1963 *Prog. Appl. Mater. Res.* **6** 117
- [2] Nabarro F R N 1986 *Strength of metals and alloys* vol 3 eds H J McQueen et al (Pergamon Press) p 1667
- [3] Gil S J 1993 *Plastic deformation and fracture of materials* ed H Mughrabi (VCH) p 19
- [4] Zehetbauer M and Seumer V 1993 *Acta Metall. Mater.* **41** 577
- [5] Nes E 1997 *Prog. Mater. Sci.* **41** 129
- [6] Kocks U F and Mecking H 2003 *Prog. Mater. Sci.* **48** 171
- [7] Kassner M and Perez-Prado M T 2000 *Prog. Mater. Sci.* **45** 1
- [8] Frost H J and Ashby M F 1982 *Deformation-Mechanisms Maps*, (Oxford: Pergamon Press)



- [9] Borner I and Eckert J 1997 *Mater. Sci. Eng.* **A226–228** 541
- [10] Zebarjad S M and Sajjadi S A 2006 *Mater. Design* **27** 684
- [11] Humphreys F J and Hatherly M 2004 *Recrystallization and related annealing phenomena* (Oxford: Elsevier)
- [12] Mecking H and Kocks U F 1981 *Acta Metall.* **29** 1865
- [13] Gottstein G and Argon A S 1987 *Acta Metall.* **35** 1261
- [14] Marthinsen K and Nes E 2001 *Mater. Sci. Technol.* **17** 376
- [15] Sandström R and Lagneborg R. 1975 *Acta Metall* **23** 387
- [16] Roucoules C, Pietrzyk M and Hodgson P D 2003 *Mater. Sci. Eng.* **A339** 1
- [17] Huang M, Rivera-D´az-del-Castillo P E J, Bouaziz O and Van der Zwaag S 2009 *Acta Mater.* **57** 3431
- [18] Hall E O 1951 *Proc. Phys. Soc. Lond.* **B64** 747
- [19] Petch N J 1953 *J. Iron Steel Inst.* **174** 25
- [20] Hansen N 2005 *Mater. Sci. Eng.* **A409** 39
- [21] Chokshi A H, Rosen A, Karch J and Gleiter H 1989 *Scr. Metall.* **23** 1679
- [22] Nieh T G and Wadsworth J 1991 *Scrip. Metall. Mater.* **25** 955
- [23] Gleiter H 2000 *Acta Mater.* **48** 1
- [24] Meyers M A, Mishra A and Benson D J 2006 *Prog. Mater. Sci.* **51** 427
- [25] Zhu Y and Langdon T G 2005 *Mater. Sci. Eng.* **A409** 234
- [26] Hahn E N and Meyers M A 2015 *Mater. Sci. Eng.* **A646** 101
- [27] Hughes D A and Hansen N 2000 *Acta Mater.* **48** 2985
- [28] Jazaeri H and Humphreys F J 2004 *Acta Mater.* **52** 3239
- [29] Huang Y and Prangnell P B 2008 *Acta Mater.* **56** 1619
- [30] Huang Y 2013 *J. Mater. Sci.* **48** 4484
- [31] Jazaeri H, Humphreys F J and Bate SP 2006 *Mater Sci Forum* **519-521** 153
- [32] Huang Y and Humphreys F J 2001 *Proc. 1<sup>st</sup> Int. Conf. on Recrystallization and Grain Growth* eds G Gottstein and D A Molodov (Springer) p 409
- [33] Zhang K, Weertman J R and Eastman JA 2005 *App. Phys. Letts.* **87** 061921
- [34] Zehetbauer M J, Steinter G, Schafner E, Korznikov A and Korznikova E 2006 *Mater. Sci. Forum* **503-504** 57
- [35] Balarin M 1975 *Phys. State Solid* **A31** 111
- [36] Hasnaoui A, Van Swygenhoven H and Derlet P M 2002 *Acta Mater.* **50** 3927
- [37] Murr L L and Hecker S S 1979 *Scrip Metall.* **3** 167
- [38] Shen Z, Wagoner R H and Clark W A T 1988 *Acta Metall.* **36** 3231
- [39] Gemperle A, Gemperlová J and Zárubová N 2004 *Mater. Sci. Eng.* **A387-389** 46
- [40] Sangid M D, Ezaz T, Sehitoglu H and Robertson I M 2011 *Acta Mater.* **59** 283
- [41] Ovid'ko L A, Sheinerman A G and Valiev R Z 2014 *Scrip. Mater.* **76** 45
- [42] Frank F C and Read Jr W T 1950 *Phys. Rev.* **79** 722
- [43] Devincere B, Hoc T and Kubin L 2008 *Science* **320** 1745